Proceedings of ICAPP '04
Pittsburgh, PA USA, June 13-17, 2004
Paper 4325

Design Development Analyses in Support of a Heatpipe-Brayton Cycle Heat Exchanger

Brian E. Steeve
NASA Marshall Space Flight Center
Huntsville, AL 35812
Tel:(256)544-7174, Fax:(256)544-7234, Email:brian.steeve@nasa.gov

Richard J. Kapernick
Los Alamos National Laboratory
Los Alamos, NM 87545
Tel:(505)665-0526, Fax:(505)665-2897, Email:rkapernick@lanl.gov

Abstract – *One of the power systems under consideration for nuclear electric propulsion or as a planetary surface power source is a heatpipe-cooled reactor coupled to a Brayton cycle. In this system, power is transferred from the heatpipes to the Brayton gas via a heat exchanger attached to the heatpipes. This paper discusses the fluid, thermal and structural analyses that were performed in support of the design of the heat exchanger to be tested in the SAFE-100 experimental program at the Marshall Space Flight Center. An important consideration throughout the design development of the heat exchanger was its capability to be utilized for higher power and temperature applications. This paper also discusses this aspect of the design and presents designs for specific applications that are under consideration.*

I. INTRODUCTION

Due to the benefits associated with its high energy density, fission power systems are being considered for in-space applications. One such system is a heatpipe reactor coupled to a Brayton cycle engine to generate electric power. To make the conversion from the reactor heat generation to electric power, the thermal energy must be transferred from the reactor to the working fluid of the Brayton cycle. This step is performed by a heat exchanger. In the heatpipe-Brayton system, the heat exchanger connects to reactor heatpipes and heats the gas mixture to the desired temperature for the Brayton cycle. The design of such a heat exchanger must consider the requirements associated with an in-space system such as high temperatures, long life, and size and weight restrictions.

An important step in the development of an in-space fission power system is the ground testing of candidate systems to evaluate and improve their designs. Because of the high costs and complexities associated with nuclear testing, these tests are proposed to be conducted using non-nuclear heating. One such test is the SAFE-100a, a 19 module, stainless steel core and heat exchanger, which has been built and will be tested at NASA's Early Flight Fission Test Facility at the Marshall Space Flight Center. Figure 1 shows how the core and heat exchanger will be configured during testing.

This paper presents the thermal, fluid, and structural analyses that have been performed in support of the heat exchanger design. The analyses have been performed for both the test model and for a possible reactor flight design. The capability of this design to be upgraded to operate at higher power levels is also discussed.

II. DESIGN DESCRIPTION

The completed heat exchanger for the SAFE-100a test is shown in Figure 2. It is an annular flow design constructed from stainless steel 316L. It is fabricated as a separate unit, pressure tested, and slid over the condenser ends of the heatpipes that extend out from the core. The assembly gaps between the heatpipes and the heat exchanger are either filled with helium or the heat

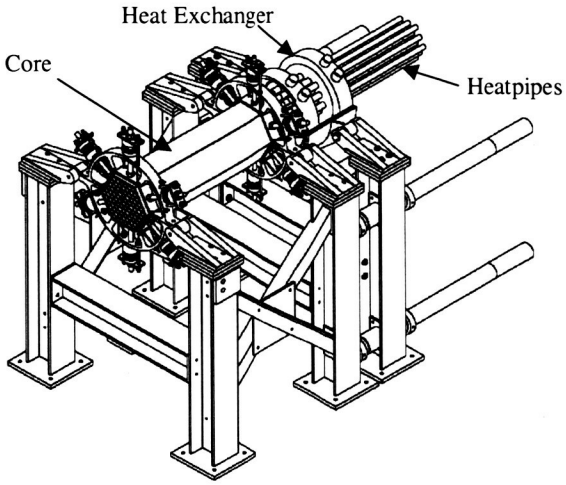

Figure 1. SAFE-100a Experimental Set-Up

exchanger is brazed to the heatpipes. Flow enters the heat exchanger at the top, passes into a flow distribution ring and crosses into the upper plenum. From there, it traverses the 19 annular flow passages, each passage surrounding a heatpipe. The flow then exits the annular flow passages, recombines in the lower plenum, crosses back into the lower flow distribution ring and then flows into the coolant return pipes.

Figure 2. SAFE-100a Heat Exchanger

Figure 3 shows the heat exchanger subcomponents. These include heatpipe sleeves, the center section block, the upper and lower flow distribution chambers, and the upper and lower cover plates. The annular flow passages are formed by the sleeves on the inside and by the circular channels in the center section block on the outside. Circular ribs are machined onto the sleeves. These ribs disrupt the boundary layer, enhancing greatly the heat transfer coefficient and ensuring turbulent flow down to a Reynolds number of about 2500.

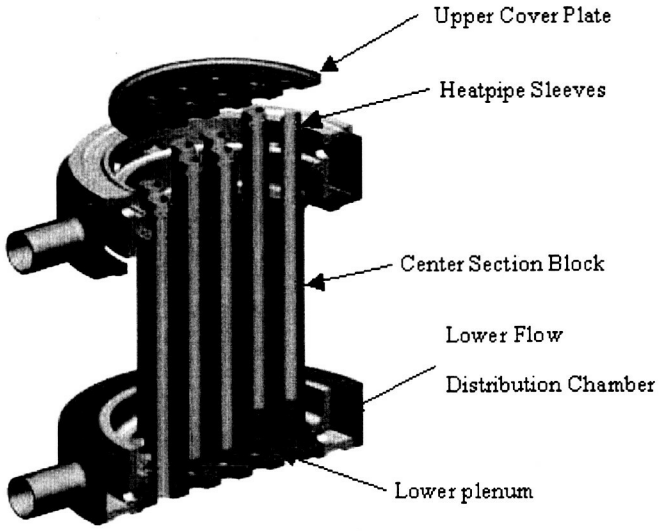

Figure 3. Partially Exploded View

The heat exchanger test model is full scale, but comprises only a partial array of heatpipe modules (19 in the test vs. 61 in the reactor). This was done to reduce the cost of the test. The use of a partial array is justified by the fact that the flow annuli in the test model, where most of the heat transfer takes place, are geometrically identical to those in the reactor heat exchanger. The dimensions of the flow distribution chamber and the height of the inlet and exit plenums have been reduced in the test model to provide approximate thermal-hydraulic similarity to the reactor heat exchanger. Further, as discussed below, CFD analyses are planned to compare flow distributions in the test and reactor models, and stress analyses have been completed for the reactor design as well as the test model. The results from these stress analyses demonstrate that the 19 heatpipe test model produces similar stress values in the critical locations in the heat exchanger.

III. FLUID AND THERMAL ANALYSIS

III.A. Test Conditions

The operating conditions that have been selected for the SAFE-100 reactor and heat exchanger are presented in Table I.

The core power level is based on mission requirements. The core dimensions are driven by the nuclear design. The coolant composition and conditions (T-in, T-out, pressure, pressure drop) are based on

recommendations from Glenn Research Center for a Brayton cycle, with the outlet temperature of 850 K taken as about the maximum envisioned for a stainless steel design. The dimensions of the heatpipe modules have been selected to produce acceptable core operating temperatures and stresses.

Table I. SAFE-100 Reactor Operating Conditions

Condition	Value
Power	100 kW
Tin	669 K
Tout	850 K
Pressure	1.38 MPa
Gas	72% He/28% Xe
No. Heatpipes	61
Heatpipe diameter	0.625in
Heatpipe pitch	1.25 in
ΔP/P	<0.025

The reactor arrangement consists of two heat exchangers attached to the heatpipes, each removing 50% of the core power. In the test, only one heat exchanger will be used, so that when the heat exchanger is operating at full power, the core will be operating at half power. This test configuration saves test costs, but also is fortuitous in that the test core operating at about 50% power produces about the same core temperatures and stresses as those in a reactor core at full power[1].

To reduce test costs, the helium/xenon mixture in the reactor Brayton system was replaced with a helium/argon mixture. A mixture of 20% helium and 80% argon was selected so that the Reynolds numbers in the test are about the same as in the reactor heat exchanger, as are dynamic heads, Mach numbers and pressure drops. However, heat transfer coefficients are about 40% lower. As a result, for the same coolant operating conditions the heatpipe and core temperatures in the test model are about 20 K higher than those in a flight reactor. This increase was considered to be acceptable.

Prior to brazing the heat exchanger to the heatpipes, a series of tests is proposed where the heat exchanger is slid on to the heatpipes and the test chamber is filled with helium. These tests will serve to assess the benefit of helium between the core modules in reducing temperatures in the event of a failed heatpipe. For these tests, the coolant temperatures will be reduced by 70 K to offset the greater temperature across the heatpipe-to-heat exchanger sleeve gap. The coolant temperature rise, which is a key driver in the heat exchanger thermal stresses, will be maintained the same at 181 K

III.B. Method

The method that has been used for the analysis of the heat exchanger is shown schematically in Figure 4. In this method, initial parametric analyses are performed using a simplified model contained in an EXCEL spreadsheet. A single annular channel is analyzed, and the channel geometry is varied to identify the optimum design that meets the design requirements. The key geometry variables are coolant channel width and length. Several performance parameters are tracked to ensure acceptable performance: heatpipe temperatures, pressure drop, Reynolds number, Mach number, and coolant velocity. The heatpipe powers vary with the core radial power distribution. To produce near-uniform coolant temperature rises in the heat exchanger coolant passages, the dimensions of the flow annuli are varied with the core radial power distribution. These calculations are also performed using the EXCEL spreadsheet.

The results from the spreadsheet analysis are used as boundary conditions for the detailed, finite element analysis using ANSYS.

For a failed heatpipe event, the coolant in the annular channel surrounding the failed heatpipe is heated only by heat transferred from surrounding heatpipes, through the connecting webs in the center section block. A SINDA/FLUINT model consisting of the failed heatpipe channel and the six surrounding channels was developed to perform this analysis. As with the EXCEL spreadsheet analysis, the results from this analysis are used as boundary conditions for follow-on, detailed finite element analysis.

The heat exchanger includes flow distribution rings at the entrance and exit, which connect to the inlet and exit plenums. The flow passages in these rings and in the plenums have been sized to provide acceptable pressure drop and flow distribution among the annular flow channels. Confirmatory analysis is performed using a CFD flow model of a symmetric half section of the heat exchanger. (This has yet to be completed).

The flow annulus includes ribs on the sleeve side to enhance heat transfer between the coolant and heatpipe. The ribs are square in cross-section, with a dimension of about 1/7 that of the channel width, and a p/h spacing of 10:1, where p is the distance between ribs and h is the rib dimension. The correlations for channel friction factor and heat transfer for this flow channel were taken from Takase[2].

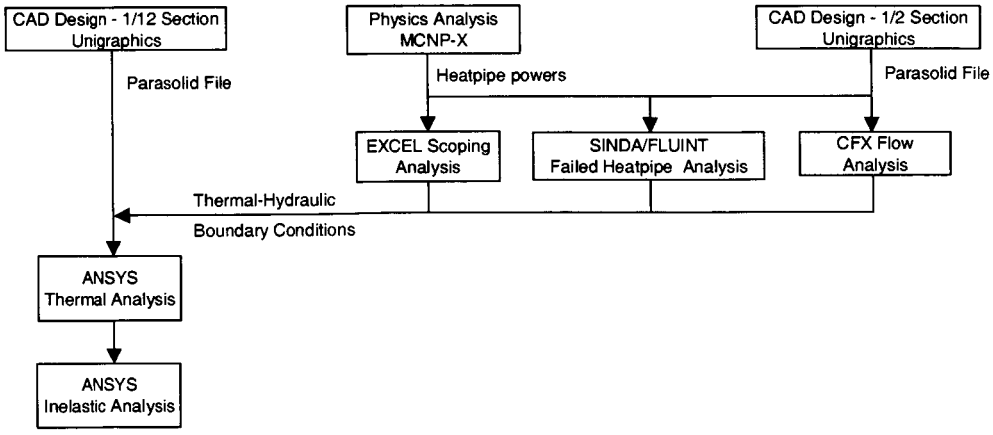

Figure 4. Heat Exchanger Thermal/Stress Analysis Procedure

III.C. Results

Results from the parametric analysis for the SAFE-100 reactor heat exchanger are shown in Figure 5. Plotted are heatpipe vapor temperatures as a function of system pressure, for a series of heat exchanger annulus lengths. For these calculations, the power and coolant temperatures

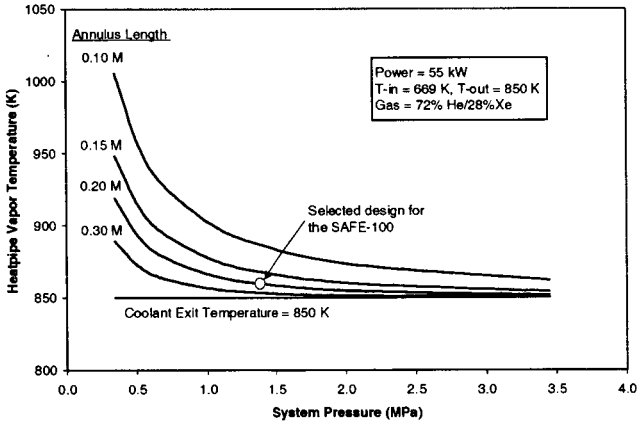

Figure 5. Heat Exchanger Parametric Study

were held constant, and a gas mixture of 72% He/28% Xe was used. For each calculation, the channel width was adjusted to produce a fractional pressure drop of DP/P = 0.015. (the pressure drop limit is ΔP/P = 0.025, but 0.01 of this limit is allocated to pressure losses in the inlet and exit plenums). As can be seen in Figure 5, heatpipe temperatures are reduced as system pressure is increased and as coolant channel length is increased. However, as the heatpipe temperature approaches the coolant temperature, the effect of increased pressure and/or increased channel length becomes small. Based on these results, a system pressure of 1.38 MPa (maximum recommended for the Brayton system) and a channel length of 0.20 m were selected for the heat exchanger design.

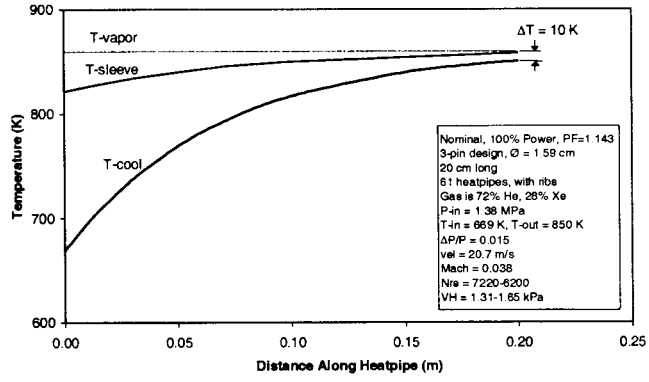

Figure 6. SAFE-100 Reactor Performance Results

Temperature profiles through the coolant flow annulus at a peak power location are presented in Figure 7. As can be seen, the temperature rise from the coolant into the heatpipe is small at the channel exit, only 10 K. Thus the heatpipe vapor temperature, which is the boundary condition temperature in the core, is close to the coolant exit temperature. The operating conditions and performance parameters for the coolant flow through this channel are also given in Figure 6. Reynold's numbers vary from over 7200 at entrance to just under 6200 at exit, and thus are turbulent. Mach number is low, and the flow is non-compressed. Coolant velocities are relatively low.

These analyses were repeated for each of the proposed test conditions, to provide input boundary conditions for the structural analyses.

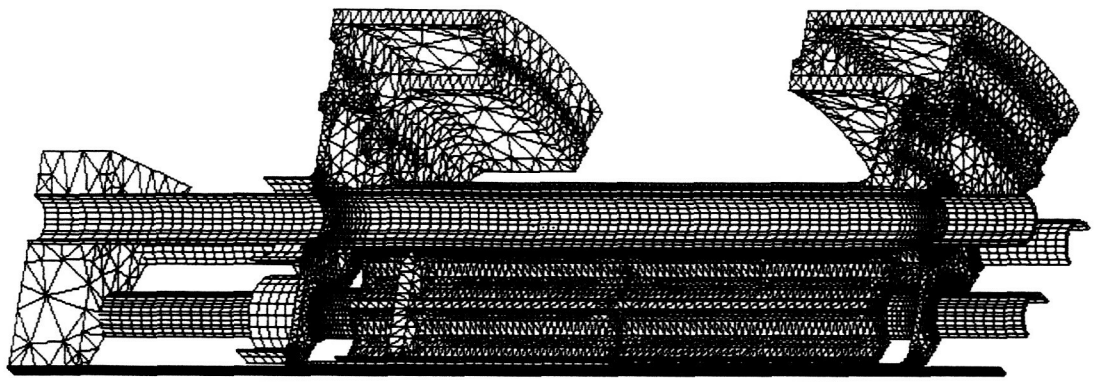

Figure 7. SAFE-100a Heat Exchanger Finite Element Model.

IV. STRUCTURAL ANALYSIS

IV.A. Method

The purpose of the structural analysis was to evaluate the heat exchanger design's ability to withstand time-independent and time-dependent failure modes under the SAFE-100a experiment pressure and thermal environments. The relevant failure modes for the heat exchanger are considered to be pressure wall burst due to overpressure or creep-rupture, and fatigue cracking due to repeated thermal cycles combined with creep effects at high temperature. A basic assumption that went into evaluating the above failure criteria is that the steady state thermal condition is the worst case and it contains the information needed to conservatively evaluate relevant failure criteria. This assumes that the startup and shutdown transients do not create stress or strain conditions that govern the failure of the heat exchanger. Making this assumption requires only a simple steady state thermal solution and only one time point to be evaluated in the structural analysis. This simplifies and reduces the scope of the analytical effort, which is desirable when evaluating many flow conditions and design configurations.

The structural analysis was performed using a finite element model. The model was built to the dimensions of the heat exchanger CAD model and represents a 1/12th slice of the heat exchanger, taking advantage of symmetry in the design. The model includes the heat exchanger, the reactor heatpipes and partial core. The model is comprised of both 10 node tetrahedron and eight node brick elements, totaling approximately 114,000 elements. The same model was used to solve for the steady state thermal solution and the structural solution, using ANSYS version 6.1. Figure 7 is a depiction of the model used in the analysis.

The SAFE-100a test series is comprised of twelve proposed test conditions. Each test condition may be run multiple times. Therefore, the structural analysis of the heat exchanger must evaluate each condition separately and then consider the lifetime capability of the heat exchanger against the expected operational life. Table II lists each test condition and its expected number of thermal cycles and hours of operation.

Table II. Proposed Test Conditions.

Test	Gap	Failed	Power	Flow	Tin	Tout	Use	
No.	Fill	HP	(kW)	(kg/s)	(K)	(K)	Cycle	Hrs
H1	He	no	27.5	0.147	760	850	14	40
H2	He	no	55	0.147	600	781	3	12
H3	He	no	65	0.174	600	781	3	12
H4	He	yes	27.5	0.147	760	850	5	16
H5	He	yes	55	0.147	600	781	3	12
H6	He	yes	65	0.174	600	781	3	12
B1	Braz	no	27.5	0.147	760	850	14	40
B2	Braz	no	55	0.147	669	850	3	12
B3	Braz	no	65	0.174	669	850	3	12
B4	Braz	yes	27.5	0.147	760	850	5	16
B5	Braz	yes	55	0.147	669	850	3	12
B6	Braz	yes	65	0.174	669	850	3	12

IV.A. Thermal Solution

The steady state thermal solution was determined from a set of thermal boundary conditions applied to the surfaces of the model. The fluid/thermal analysis

described above provided the heat transfer coefficients and bulk fluid temperatures in each annular flow channel and in the inlet and outlet manifolds. The exterior of the heat exchanger and heatpipe sections between the core and heat exchanger were assumed to be adiabatic. With the thermal boundary conditions applied, the temperature profile was solved for each test condition for input into the structural analysis.

IV.A. Structural Solution

The loadings for the structural solution consist of a thermal profile from the thermal analyses and an internal pressure of 1.38 MPa. In addition to the symmetry boundary conditions on the radial planes, the core and heat exchanger were restrained axially and the heatpipes were allowed to freely grow in the axial direction. Each test condition was then run to solve for the steady state stress and strain profiles.

The thermal profiles for each load case were high enough that they induced localized plastic strains. Therefore each case was run with temperature dependent bilinear stress-strain material models. The solution was then solved non-linearly. Some of the load cases were also run elastically to calculate stresses due only to the pressure loading. For these cases, the coefficient of thermal expansion was set to zero to remove the thermal stress.

IV.A. Structural Criteria

The structural criteria applied to the design of the SAFE-100a HX have been derived from the American Society of Mechanical Engineers (ASME) Boiler and Pressure Vessel Code (BPVC) Section III, Division 1 - Subsection NH[3]. This subsection applies to pressurized components at elevated temperatures where creep effects are significant. Three basic criteria have been taken from the code to address the burst and fatigue failure modes. They are load controlled stresses, total lifetime inelastic strains, and combined creep-fatigue damage.

The load-controlled stress criteria are the rules found in the Subsection NH-3222 of the BPVC for Level A and B service levels. These criteria are used to ensure that no short-term strength or long-term creep-induced failure occurs due to the pressure load. The criteria are based upon membrane and bending stress intensity through a section and are limited by allowable time-independent and time-dependent stresses given in the code for 316 stainless steel. The thermal stresses are not included in this criterion since they are displacement controlled and do not contribute to an overstress type of failure.

The inelastic strain criteria are taken from Appendix T-1310 of Subsection NH and limit the maximum lifetime allowable local strain, including all plasticity and creep effects. The limits are 1% average strain through a section, 2% strain at the surface due to an equivalent linearized strain through a section, and 5% peak strain at a point based upon the maximum positive principle strain.

The creep-fatigue damage criterion is intended to assess mircrostructural damage than can occur due to repeated loading and creep mechanisms and eventually lead to crack initiation. The criterion is from Appendix T-1411 and is summarized below. The total allowable damage, D, for 316L stainless steel is given by the graph in Figure 8.

$$\sum_{j=1}^{p}\left(\frac{n}{N_d}\right)_j + \sum_{k=1}^{q}\left(\frac{\Delta t}{T_d}\right)_k \le D$$

Fatigue Ratio — Creep Ratio

Where:

- n = number of applied cycles for cycle type j
- N_d = Number of allowable cycles for cycle type j based on low cycle fatigue life
- Δt = duration of the time interval k
- T_d = allowable time duration for time interval k based on stress-to-rupture

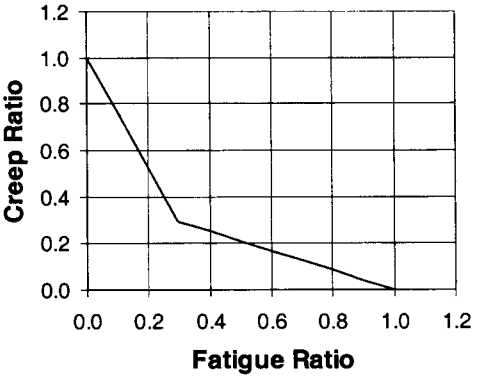

Figure 8. Allowable Creep-Fatigue Damage Ratio for 316L Stainless Steel

The criteria used for welds and the surrounding heat affected zones are the same as above except that lower allowables are used per the ASME Code. The allowables for the load-controlled stress do not change for 316 stainless steel but the allowable maximum inelastic strain levels are one-half the allowable for non-welded regions. The number of allowable fatigue cycles is one-half that of the parent material and the stress-to-rupture allowables are reduced a few percent for the creep-fatigue criteria.

IV.A. Results

The analysis for the SAFE-100a test model involved running the steady state thermal and structural solution for the twelve proposed test conditions. The stresses and strains from each case were then checked against the design criteria. Since the time for each test is relatively short (less than 10 hours), the effect of stress relaxation due to creep was not included. The short test times and numerous cycles act to make the life of the heat exchanger fatigue dominated.

The stresses due to the internal pressure are essentially the same for all of the test conditions, and are shown in Figure 9. The peak stress occurs in the cover plates between the outer heatpipes and the outside edge weld where the unsupported span in the largest. The load controlled criteria are based upon the membrane and bending stresses through a section. In the analyses these stresses were extracted from the model at the peak stress intensity locations of each part. The results show that the stresses are below the ASME Code strength allowables and allow for greater than 100,000 hours of creep life.

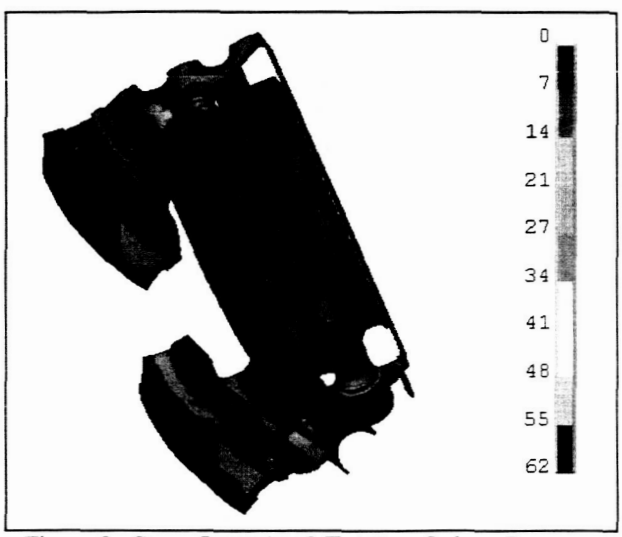

Figure 9. Stress Intensity (MPa) Due Only to Pressure.

The temperature variations in the heat exchanger cause significant thermal stress to develop. The stress in some areas is above the material yield strength so that plastic strains develop in localized regions. These regions are primarily around the weld joints at the ends of the sleeves, therefore the criteria for welds are used. The strains in these regions are the critical factor determining the lifetime capability of the heat exchanger. The failed heatpipe cases are the most severe due to the large temperature difference between the failed heatpipe and the adjacent heatpipe. Figure 10 shows the temperature profile for a failed heatpipe condition.

Within the localized plastic regions, the maximum principle strain is within the inelastic strain criteria for all of the test conditions. The failed heatpipe conditions generate the highest strain levels. Figure 11 shows the peak strains occurring in the center failed heatpipe sleeve on the inlet side.

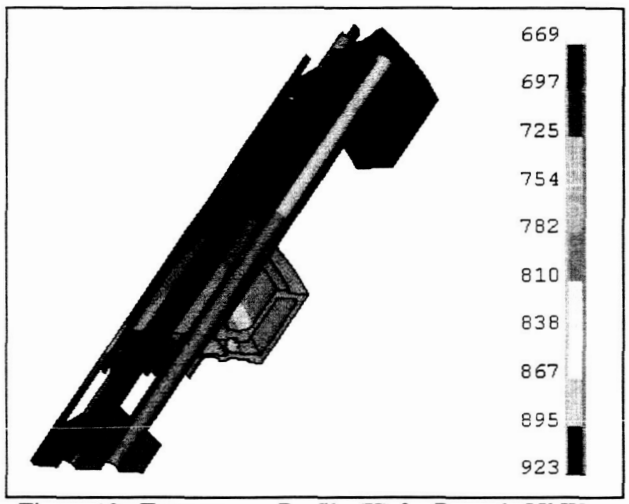

Figure 10. Temperature Profile (K) for Brazed, 55kW, Failed Heatpipe Condition.

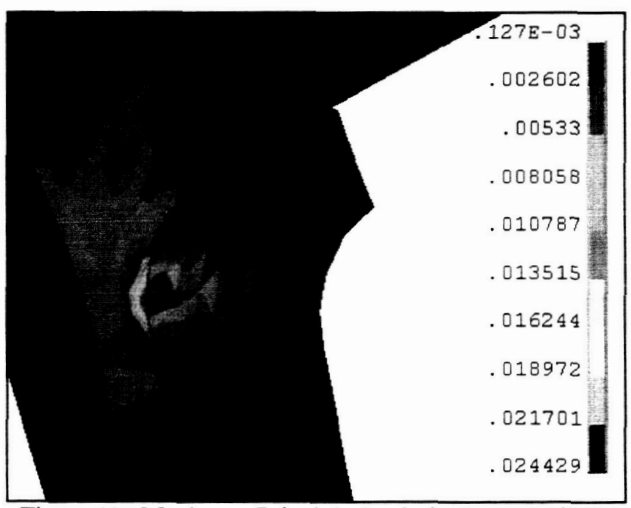

Figure 11. Maximum Principle Strain in Center Failed Heatpipe Sleeve.

The creep-fatigue limit requires knowledge of the temperature, stress, and strain state at a given point. For this analysis, the three nodes in the heat exchanger corresponding to the maximum temperature, equivalent total strain, and Von Mises stress were used to calculate an allowable number of cycles and creep lifetime at each node. These nodes were generally at different locations from test to test. Therefore, this is a somewhat

conservative application of the criteria. The ratio of the expected usage listed in Table 2 to the allowable number of fatigue cycles and creep hours for each test condition were then summed to determine the total damage. Figure 12 plots the maximum damage locations against the allowable damage ratio for 316L stainless steel. The most damage occurs in the center sleeve and is assumed to occur in the sleeve to cover plate weld so the weld creep-fatigue criteria are used.

Nearly all of the fatigue and creep damage occurs during the failed heatpipe tests. Figure 13 shows that the maximum strain levels in the failed heatpipe tests are from 2-18 times greater than the non-failed heatpipe tests. Additional non-failed heatpipe test cycles could be added to the test series with negligible impact to the heat exchanger creep-fatigue damage.

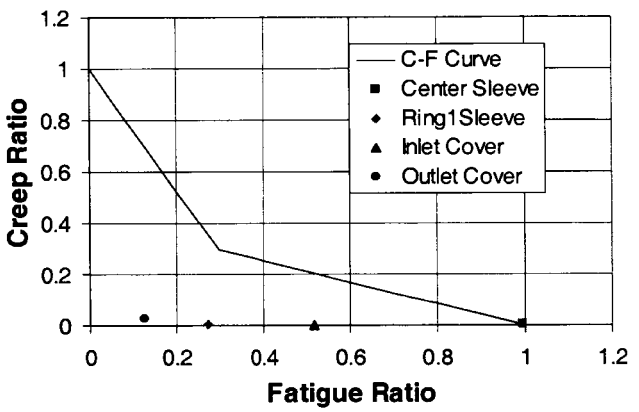

Figure 12. Creep-Fatigue Damage Results

An analysis of the test model but using flight reactor thermal conditions was also performed. One purpose of this analysis is to compare with the test model results for similarity in performance, to show how well the SAFE-100a tests represent the structural behavior of a flight unit. The results indicate that the temperature of the reactor is a few degrees cooler and the reactor stress and strain is similar to the tests. Figure 14 plots the stress for a few select nodes representing the peak damage locations from the reactor for both the SAFE-100a test and reactor conditions. The reactor stress tracks the test results fairly well indicating the tests are a good representation of the reactor behavior.

Another purpose of the reactor analysis was to investigate the stress relaxation effects due to creep over a long mission life, since a flight reactor could be expected to operate for several years. Creep properties for 316L stainless steel were included in the test model. The model was then run with the reactor conditions for several time points up to 50,000 hours. All of the strain due to coolant pressure, as well as temperature differences, was included in the first time point.

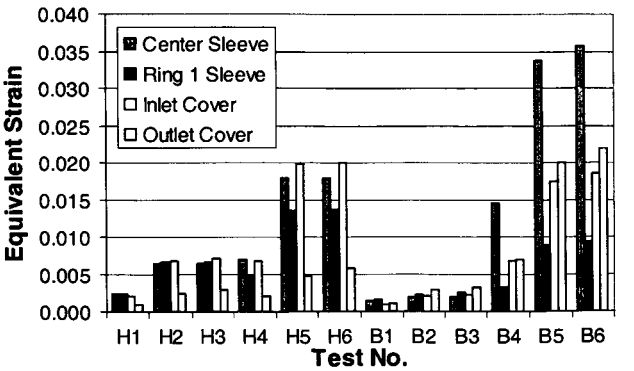

Figure 13. Maximum Strains for Each Test Condition

The creep effects are greatest in the hot outlet side of the heat exchanger. The critical locations are again in localized inelastic regions around the sleeve to cover plate welds. The equivalent stress and strain for a peak point in the outlet cover plate are plotted vs. time in Figure 15. Results from both a non-failed heatpipe and failed heatpipe condition are included. The creep effects are not significant at times less than 100 hours. Beyond 100 hours significant strain levels begin to accumulate and the stress state experiences significant relaxation. These results serve to confirm the decision to neglect creep effects for the short duration tests.

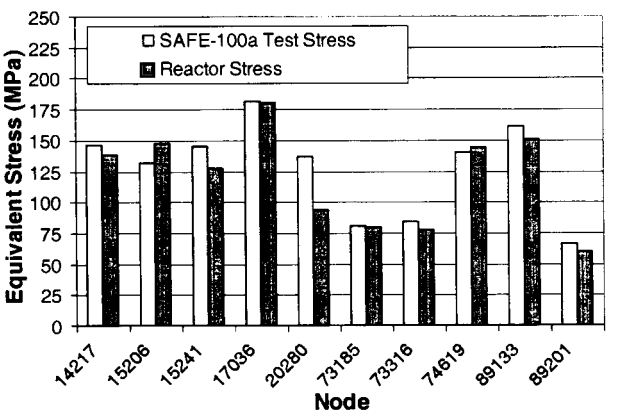

Figure 14. Reactor and Test Stress Comparison

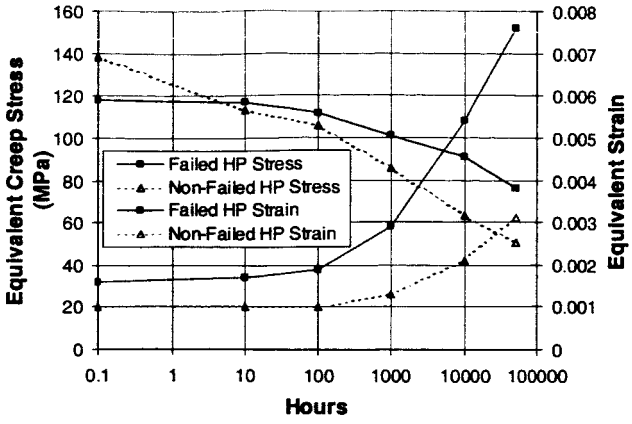

Figure 15. Stress Relaxation of Reactor Core in the Outlet Cover Plate

V. HEAT EXCHANGER POWER INCREASE POTENTIAL

There are several parameters that affect the amount of power that can be transferred in the heat exchanger. These include module dimensions and number of modules, heatpipe vapor temperature, heat exchanger temperature and stress limits, coolant pressure and pressure drop, coolant inlet and exit temperatures, and coolant gas constituents. For the SAFE-100 design many of these parameters were considered to be fixed, either by the nuclear design or the Brayton system requirements. In this study, only the heatpipe vapor temperature (and its effect on heat exchanger temperatures) was varied. For each case, the coolant annulus dimensions (width and length) were adjusted to achieve the desired heatpipe vapor temperature and a pressure drop of $\Delta P/P=0.015$ in the annulus.

The results of this analysis are shown in Figure 16 for heatpipe vapor temperatures varying from 860 K (SAFE-100 reactor design temperature) to 900 K, and for heat exchanger powers of 55 kW (SAFE-100 heat exchanger power) to 200 kW. The two parameters plotted are length of flow annulus and the spacing between adjacent flow channels. The length is important as it affects the size and weight of the heat exchanger. The spacing between adjacent flow annulus jackets provides an ultimate limit in the heat exchanger power: at a high enough power, this distance becomes zero and further increases in power are not possible without changing one or more of the operating parameters that were fixed in this analysis.

The heatpipe vapor temperature is important because it provides the boundary condition temperature for the reactor core. This temperature is increased by shortening the annulus length (decreasing heat transfer area), which in turn decreases the annulus width needed to meet pressure drop and increases the spacing between adjacent flow annuli. The Figure 16 results show that the SAFE-100 heat exchanger is capable of much higher power levels. It should be noted that these increases in power do not increase appreciably the stresses in the heat exchanger. The key drivers of stress in the heat exchanger are coolant temperature rise and coolant pressure, which are being held constant.

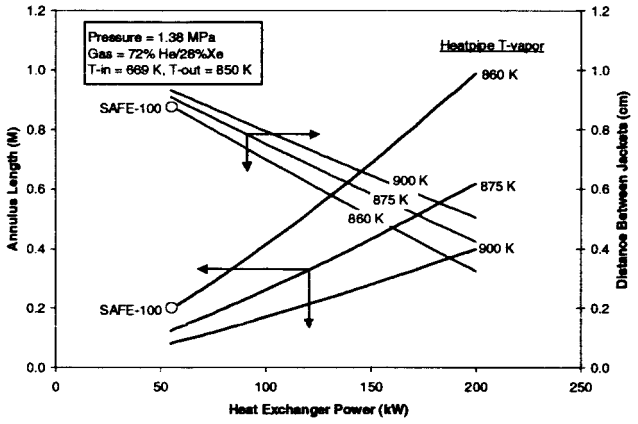

Figure 16. Heat Exchanger Power Increase Assessment

However, at higher powers the heat exchanger becomes long, so that changes to reduce length should be assessed. In addition to allowing the heatpipe vapor temperature to increase, these include a larger temperature rise, higher coolant pressure and/or a gas mixture with a higher mole fraction of helium. The increases in coolant pressure and coolant temperature rise would increase heat exchanger stress, which would need to be evaluated. If needed, increases in temperatures could be offset by a reduction in coolant temperatures, with some attendant loss in Brayton cycle efficiency.

VI. CONCLUSIONS

The structural performance of the heat exchanger is driven by the thermal stress and strain. The sleeve to cover plate weld regions are the most critical locations because of the peak localized stresses and the lower weld allowables. This makes the quality of these welds an important manufacturing issue.

For the SAFE-100a test series, the heat exchanger meets the strength criteria of the ASME Pressure Vessel and Boiler Code.

The SAFE-100a test environment produces a stress-strain state that is similar to the reactor conditions. The tests are therefore a good simulation for a flight unit. The

analytical techniques developed for the SAFE-100a tests can now be used to support the tailoring of the heat exchanger design to meet the requirements of a long mission life.

Should a mission require a reactor power greater than 100 kW, this same heat exchanger design could still be used up to certain physical limits by adjusting the annulus length, width, and/or heatpipe vapor temperature. This can be done without altering the pressure and coolant temperature.

REFERENCES

1. R. J. KAPERNICK and R. Guffee, "Thermal Stress Calculations for Heatpipe-Cooled Reactor Power Systems," *Proc. of the Space Technology and Applications Int. Forum (STAIF-2003), AIP Conference Proceedings,* Vol. 654, pp. 457-465, American Institute of Physics, New York, USA (2003).

2. K. TAKASE, "Forced Convection Heat Transfer in Square-Ribbed Coolant Channels with Helium Gas for Fusion Reactors," *Fusion Engineering and Design,* Vol. 49-50, pp. 349-354 (2000).

3. ASME, *Boiler and Pressure Vessel Code, Section III, Division 1, Subsection NH, Class 1 Components in Elevated Temperature Service*, ASME, New York (2001).